Polymer 51 (2010) 1639–1647

Contents lists available at ScienceDirect

Polymer

journal homepage: www.elsevier.com/locate/polymer

Crystallization of poly(L-lactide-dimethyl siloxane-L-lactide) triblock copolymers and its effect on morphology of microphase separation

Chang-Hong Ho [a], Guang-Way Jang [b], Yu-Der Lee [a,*]

[a] Department of Chemical Engineering, National Tsing Hua University, Hsinchu, 30013, Taiwan
[b] Industrial Technology Research Institute, Hsinchu, 30013, Taiwan

ARTICLE INFO

Article history:
Received 25 August 2009
Received in revised form
13 October 2009
Accepted 13 November 2009
Available online 17 November 2009

Keywords:
Microphase separation
Poly(L-lactide)
Poly(dimethyl siloxane)

ABSTRACT

This investigation characterizes the molten morphologies following isothermal crystallization of poly(L-lactide-*block*-dimethyl siloxane-*block*-L-lactide) triblock copolymers, which were synthesized by ring-opening polymerization of L-lactide using hydroxyl-telechelic PDMS as macroinitiators, via small-angle X-ray scattering (SAXS) and transmission electron microscopy (TEM). The break-out and preservation of the nanostructure of the triblock copolymer depended on the segregation strength, which was manipulated by varying the degree of polymerization. The crystallization kinetics of these semicrystalline copolymers and the effect of isothermal crystallization on their melting behaviors were also studied using DSC, FT-IR and WAXS. The exclusive presence of α-phase PLLA crystallite was verified by identifying the absence of the WAXS diffraction signal at $2\theta = 24.5^\circ$ and the presence of IR absorption at 1749 cm^{-1} when the PLLA segment of the *block* copolymers was present as a minor component. The dependence of the crystallization rate (Rc) on the chemical composition of the triblock copolymers reveals that the Rc of the triblock copolymers was lower than that of PLLA homopolymer and the Rc were substantially reduced when the minor component of the crystallizable PLLA domains was dispersed in the PDMS matrix.

1. Introduction

Block copolymers that consist of at least two blocks of chemically different monomers can self-assembly into various periodic nanostructures in bulk, depending on the segregation strength χN, where χ and N represent the Flory–Huggins interaction parameter and the degree of polymerization, respectively, and the volume ratio of the constituent components. Incorporating crystallizable moieties within the block copolymers has attracted great interest because of the kinetic complexity in the self-assembly process and the morphological richness. The morphologies of semicrystalline block copolymers are determined by two factors: the thermodynamical incompatibility between the constituent blocks and the crystallization of the crystallizable blocks [1–19]. In general, the structure development has been found to be path-dependent and can typically be categorized as follows based on the correlation between melting temperature (T_m), order-disorder transition temperature (T_{ODT}) of block copolymers and glass transition temperature (T_g) of the amorphous blocks. For $T_C > T_{ODT} > T_g$ [5,13], the formation of nanostructures is induced by crystallization and lamellar structures were formed. In cases of hard confinement with $T_{ODT} > T_g > T_c$ [1,3,7,9,13,16,18,20,21], the ordered structures are preserved by the vitreous domains. In contrast, the morphologies under the soft confinement conditions with $T_{ODT} > T_c > T_g$ depend on the segregation strength of the block copolymers [3–14,18,21].

Polylactide (PLA) is an environmentally friendly aliphatic polyester and has been emerging as an alternative to conventional petroleum-based polymeric materials because of its renewability, biodegradability and greenhouse gas neutrality. PLA is typically synthesized by the ring-opening polymerization of lactide. The properties of the PLA depend on the chirality: poly(L-lactide) (PLLA) or poly(D-lactide) (PDLA) with high optical purity are semicrystalline ($T_g \sim 60\ ^\circ C$, $T_m \sim 180\ ^\circ C$) while poly(D,L-lactide) (PDLLA) is amorphous ($T_g \sim 60\ ^\circ C$) [22,23]. Although PLA is a high-strength and high-modulus polymer that is analogous to polystyrene, the inherent brittleness and low toughness of polylactide in its pristine state restrict its range of applications, and the toughening of PLLA by the blending method and copolymerization strategy have been studied [24–27].

The intriguing properties of poly(dimethyl siloxane) (PDMS), including high thermal and electrical stability, low surface energy, high gas permeability, low glass transition temperature and low

* Corresponding author. Tel.: +886 3 5713204; fax: +886 3 5715408.
E-mail address: ydlee@che.nthu.edu.tw (Y.-D. Lee).

0032-3861/$ – see front matter © 2009 Elsevier Ltd. All rights reserved.
doi:10.1016/j.polymer.2009.11.030

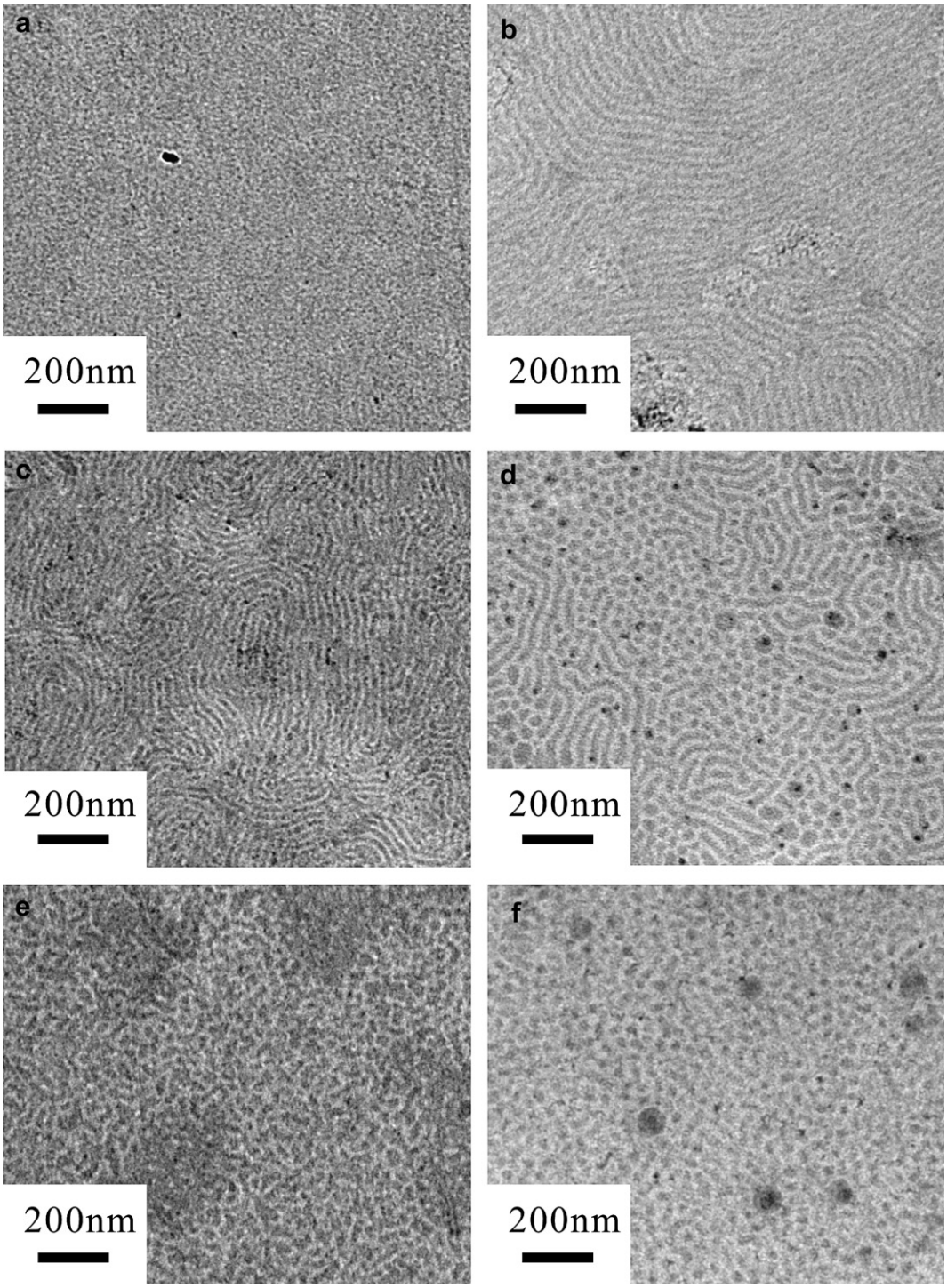

Fig. 1. TEM micrographs of PLLA–PDMS–PLLA triblock copolymers quenched from the molten state. (a) $La_{25}DM_{50}La_{25}$; (b) $La_{45}DM_{50}La_{45}$; (c) $La_{60}DM_{50}La_{60}$; (d) $La_{70}DM_{50}La_{70}$; (e) $La_{40}DM_{130}La_{40}$; (f) $La_{220}DM_{100}La_{220}$.

toxicity, make PDMS useful in many fields, such as elastomers, biomaterials, electronics, microlithography and others. In previous investigations, triblock copolymers that contain PLLA and PDMS were utilized as polymer probes [28] and magnetite nanoparticle dispersants [29]. Studies of PLLA/PDLA stereocomplexation [30] were also repoerted. In the authors' previous research [31], highly-mobile hydrophobic PDMS segments were introduced into PLLA to modify the mechanical properties of PLLA, and the microphase separation of PLLA–PDMS–PLLA triblock copolymers was identified using differential scanning calorimetry (DSC) and dynamic mechanical analysis (DMA) for the first time. However, the nano-structures have not been investigated.

In this study, the morphologies of amorphous-semicrystalline PLLA–PDMS–PLLA triblock copolymers with various compositions and the effect of isothermal crystallization on the development of their morphologies were characterized by transmission electron microscopy (TEM) and small-angle X-ray scattering (SAXS). The isothermal crystallization of the block copolymers was examined

Table 1
Related data of PLLA–PDMS–PLLA triblock copolymers.

Entry[a]	Mw_{NMR}[b]	W_{PLLA}[c]	Tg $_{PLLA}$	Tg $_{PDMS}$	f_{PLLA}[d]	PDI	Morphology	T_m^0[e]
$La_{25}DM_{50}La_{25}$	9613	0.48	33.6	−125.0	0.43	1.25	Disordered	150.4
$La_{45}DM_{50}La_{45}$	13,925	0.64	45.2	−119.4	0.56	1.31	Lamella	176.3
$La_{60}DM_{50}La_{60}$	16,510	0.70	53.3	−119.0	0.64	1.27	Cylinder	180.9
$La_{70}DM_{50}La_{70}$	18,087	0.73	55.9	−118.5	0.67	1.31	Cylinder	181.6
$La_{40}DM_{130}La_{40}$	20,258	0.37	48.9	−115.3	0.31	1.32	Cylinder	156.3
$La_{220}DM_{100}La_{220}$	52,082	0.81	60.3	−112.3	0.76	1.30	Sphere	185.5

[a] La and DM represent the poly(L-lactide) and poly(dimethyl siloxane) segments, respectively, and the number is the molecular weight of each chain length.
[b] The molecular weight of triblock copolymers was determined from ^{1}H NMR.
[c] Weight fraction of PLLA in the triblock copolymers was calculated from the molecular weight of constituent segments determined by ^{1}H NMR.
[d] Volumetric ratio of PLLA in the triblock copolymer was calculated by the following equation, $f_{PLLA} = (W_{PLLA}/d_{PLLA})/(W_{PLLA}/d_{PLLA}) + [(1 - W_{PLLA})/d_{PLLA}]$, where density of PLLA (d_{PLLA}) was 1.248 g/cm^3 [17], and density of PDMS (d_{PDMS}) was 0.98 g/cm^3, obtained from the released technique date from ShinEtsu Chemical Co. Ltd.
[e] T_m^0 is the equilibrium melting temperature.

using DSC, and the dependence of the composition on the crystallization kinetics rate (Rc), was also discussed. The effect of crystallization temperature (T_c) and the chemical composition of the block copolymers on the melting behavior and crystallite structure of PLLA segments were studied by FT-IR, DSC and wide-angle X-ray scattering (WAXS).

2. Experimental

2.1. Materials

Bis(2-hydroxy ethyl propyl ether) terminated poly(dimethyl siloxane) with a M_w of 4953 (g/mol.), which was served as a macroinitiator for the synthesis of triblock copolymers, was purchased from ShinEtsu Chemical Co. Ltd. L-lactide from Bio Invigor Co., Taiwan was recrystallized from HPLC-grade acetone and stored in dry nitrogen atmosphere after it was dried under reduced pressure at 60 °C. Toluene was dried by refluxing in the presence of sodium metal in a nitrogen atmosphere. Oxalyl chloride, pyridine, 0.5 wt% aqueous ruthenium tetroxide (RuO_4) and tin octoate obtained from Sigma–Aldrich were used without further treatment.

2.2. Extension of chain length of hydroxyl-terminated poly(dimethyl siloxane)

To increase the M_w of hydroxyl-terminated poly(dimethyl siloxane), excess PDMS was coupled with oxalyl chloride as follows: viscous PDMS fluid was charged into a two-neck round bottom flask connected to a vacuum line system, and the atmosphere was replaced with dry nitrogen. After 0.8 molar equivalents of oxalyl chloride had been added, the reaction mixture was stirred at room temperature for at least 12 h, and then titrated with pyridine. The cloudy solution was filtrated through a flash column that was packed with celite 545. The obtained transparent filtrate was further precipitated in methanol, and then dried at 60 °C under reduced pressure. The molecular weight of PDMS was estimated using the following equation:

$$Mw_{PDMS} = \frac{\left(A_{\delta=0ppm}/6\right)}{\left(A_{\delta=2.0ppm}/2\right)} \times 75$$

where $A_{\delta=0}$ and $A_{\delta=2..0}$ represents the area of ^{1}H NMR signal of CH_3 groups of dimethyl siloxane units and the hydrogen of terminal hydroxyl groups, respectively, and value of 75 is the molecular weight of repeat units of poly(dimethyl siloxane). Two specimens of PDMS with molecular weight of 10,000 and 13,000 (g/mol), respectively, were obtained.

2.3. Synthesis of PLLA–PDMS–PLLA triblock copolymers

The triblock copolymers PLLA–PDMS–PLLA utilized in the study were prepared by ring-opening polymerization of L-lactide using hydroxyl-telechelic poly(dimethyl siloxane) as macroinitiator. The detailed procedure was referred to the synthetic method described in the literature [31]. Briefly, the desired amounts of PDMS and L-lactide were added to a two-necked round bottom flask equipped with a condenser. The solution polymerization in toluene proceeded at 140 °C for 6 h upon addition of tin octoate. After the suspension in the product solution was removed, further purification was conducted by precipitating the polymer solution in methanol. All of the specimens were named as LaxxDMyyLaxx based on the constituent component and the chain length in the block copolymers, where La and DM represent the PLLA and PDMS blocks, respectively, and xx and yy denote the molecular weight of the respective segment. The molecular weight of the triblock copolymer was determined using ^{1}H NMR and calculated by the following equation:

$$M_{wtri} = Mw_{PDMS} + 72 \times \frac{A_{\delta=5.1ppm}}{A_{\delta=3.4ppm}/4}$$

where $A_{\delta=5.1ppm}$ and $A_{\delta=3.4ppm}$ represent the area of the ^{1}H NMR signal of PLLA methine hydrogen at $\delta = 5.1$ ppm and and that of PDMS methylene hydrogen at 3.4 ppm, respectively. The value of 72 was the molecular weight of the repeating units of PLLA.

2.4. Structure characterization

The structures of the PLLA–PDMS–PLLA triblock copolymers were verified by proton nuclear magnetic resonance spectroscopy (^{1}H NMR), using d-chloroform as solvent, and the Fourier transform infrared spectroscopy (FT-IR). The IR spectra were recorded in the range of 500–4400 cm^{-1} with a resolution of 2 cm^{-1} using a PerkinElmer EX 1 FT-IR equipped with a PIKE MIRacle™ Single Reflection ATR; 16 scans were made for each specimen.

2.5. Thermal analysis

The thermal properties of triblock copolymers were measured using a PerkinElmer's Diamond DSC instrument equipped with an automatic liquid nitrogen cooling system (CryoFill) or with a water cooling circulator. Three standards, including cyclopentane with transition temperature at −132 °C, water at 0 °C and indium metal at 156 °C, were employed to calibrate the temperature. The enthalpy was calibrated with reference to the heat of fusion of indium. All of the measurements were made in the nitrogen atmosphere. The procedure for isothermal crystallization

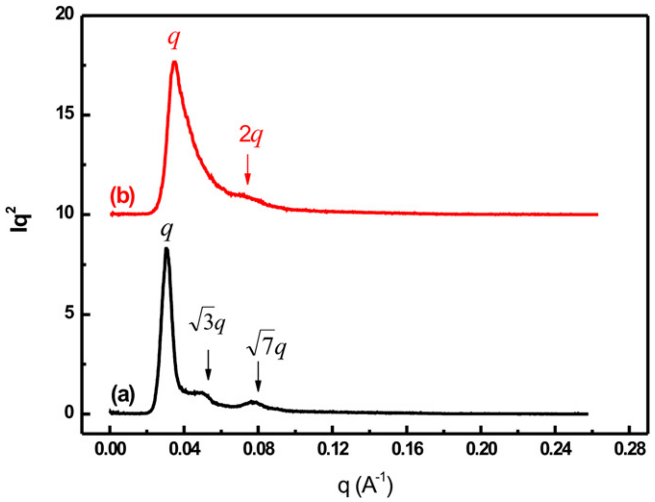

Fig. 2. SAXS profiles for $La_{60}DM_{50}La_{60}$ triblock copolymers (a) in the melting state; (b) isothermal crystallized at 120 °C for 30 min.

experiment was described as follows. First, 3–5 mg of specimens was sealed in the aluminum pan. The sample was heated to 185 °C and kept at constant for 3 min to erase its thermal history. Then, it was immediately cooled to the designated T_c at a cooling rate of 50 °C/min and the heat flow was recorded as a function of time until it remained constant. Subsequently, the sample was further heated from T_c to 185 °C at a heating rate of 10 °C/min to record the melting behaviors following the isothermal crystallization.

2.6. Transmission electron microscopy

The bright-field electron micrographs of the morphologies of PLLA–PDMS–PLLA triblock copolymers were obtained using mass-thickness contrast with a JEOL-2100 (HT) TEM transmission electron microscope operated at an acceleration voltage of 120 kV. The specimens were prepared as follows. A polymer solution in THF with a concentration of 1.0 wt% was formulated and filtered through a 0.45 μm syringe filter. After the solution was dropped into a deionized water bath, the polymer thin film that was floating on the surface of water was collected by a 200 mesh copper grid coated with the carbon film, and then dried in the vacuum oven at 60 °C overnight. To enhance the contrast of TEM image, the specimens were further vapor-stained with RuO4 (0.5 wt% aqueous solution) for 3 min, and then coated with a thin layer of carbon film in the high-vacuum evaporator.

2.7. Wide angle and small-angle X-ray scattering experiments

Small-angle X-ray scattering (SAXS) experiments were performed using an Osmic PSAXS-USH-WAXS-002, USA, at National Taiwan University of Science and Technology, Taiwan. The SAXS intensities obtained were plotted against scattering vector $q = (4\pi/\lambda)\sin\theta$, where λ is the wavelength of the X-ray ($\lambda = 0.154$ nm) and 2θ is the scattering angle. The beam center was calibrated using silver behenate. A Rigaku Ultima IV X-ray diffractometer system was applied to measure the wide-angle X-ray scattering (WAXS) patterns of triblock copolymers. The X-ray beam was Cu Kα radiation. The WAXS analysis of the PLLA that was crystallized at various T_c was measured in the 2θ range of 5–40° at a scanning rate of 2°/min at room temperature.

3. Results and discussion

3.1. Morphology of triblock copolymers in melting state

In the authors' previous work [31], PLLA–PDMS–PLLA triblock copolymers with two distinct glass transition temperatures (T_g) of −122 ~ −120 °C and 30–50 °C, determined by DSC and dynamic mechanical analyzer (DMA) and consistent with the T_g of PDMS and PLLA segments, respectively, manifested the occurrence of microphase separation in the PLLA–PDMS–PLLA triblock copolymers because of the difference between the solubility parameters of the constituent segments. The bulk morphologies of the triblock copolymers containing crystallizable PLLA segments were examined in this research. To eliminate the effect of PLLA crystallization on the bulk nanostructure in the melt, the specimens were melted at 10 °C above the Tm of PLLA segments for 3 min and then immediately immersed into the liquid nitrogen bath to trap morphologies in the molten state. Fig. 1 displays the bulk morphologies of triblock copolymers comprising various chemical compositions, including $La_{40}DM_{130}La_{40}$ with the PDMS as the matrix as well as others with PLLA as the major component. Table 1 presents the related data of triblock copolymers. Since silicon in

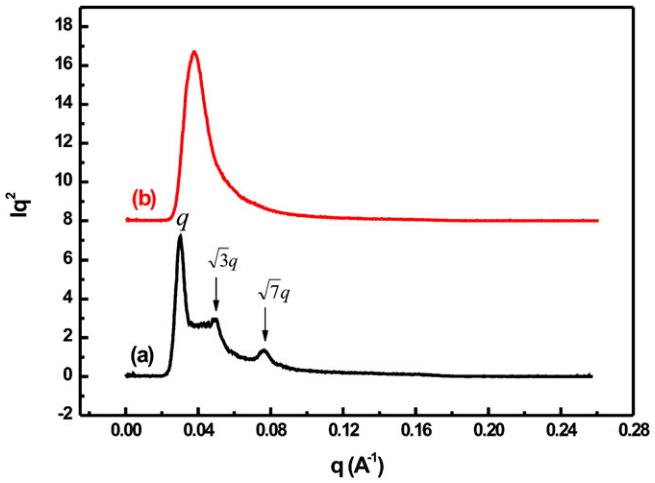

Fig. 3. SAXS profiles for $La_{70}DM_{50}La_{70}$ triblock copolymers (a) in the melting state; (b) isothermal crystallized at 120 °C for 30 min.

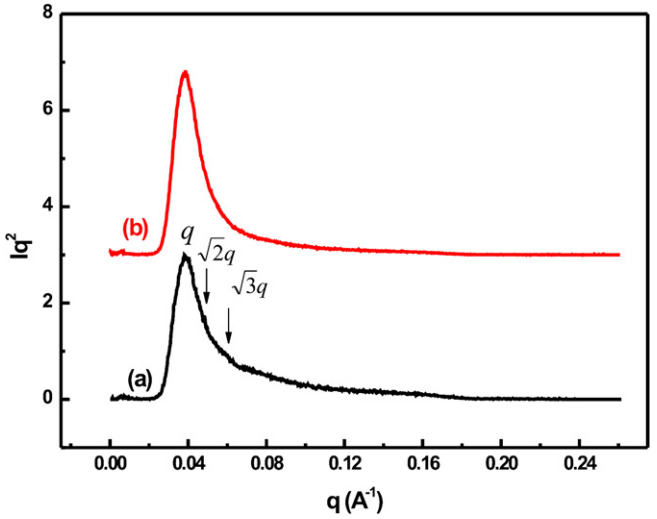

Fig. 4. SAXS profiles for $La_{220}DM_{100}La_{220}$ triblock copolymers (a) in the melting state; (b) isothermal crystallized at 140 °C for 120 min.

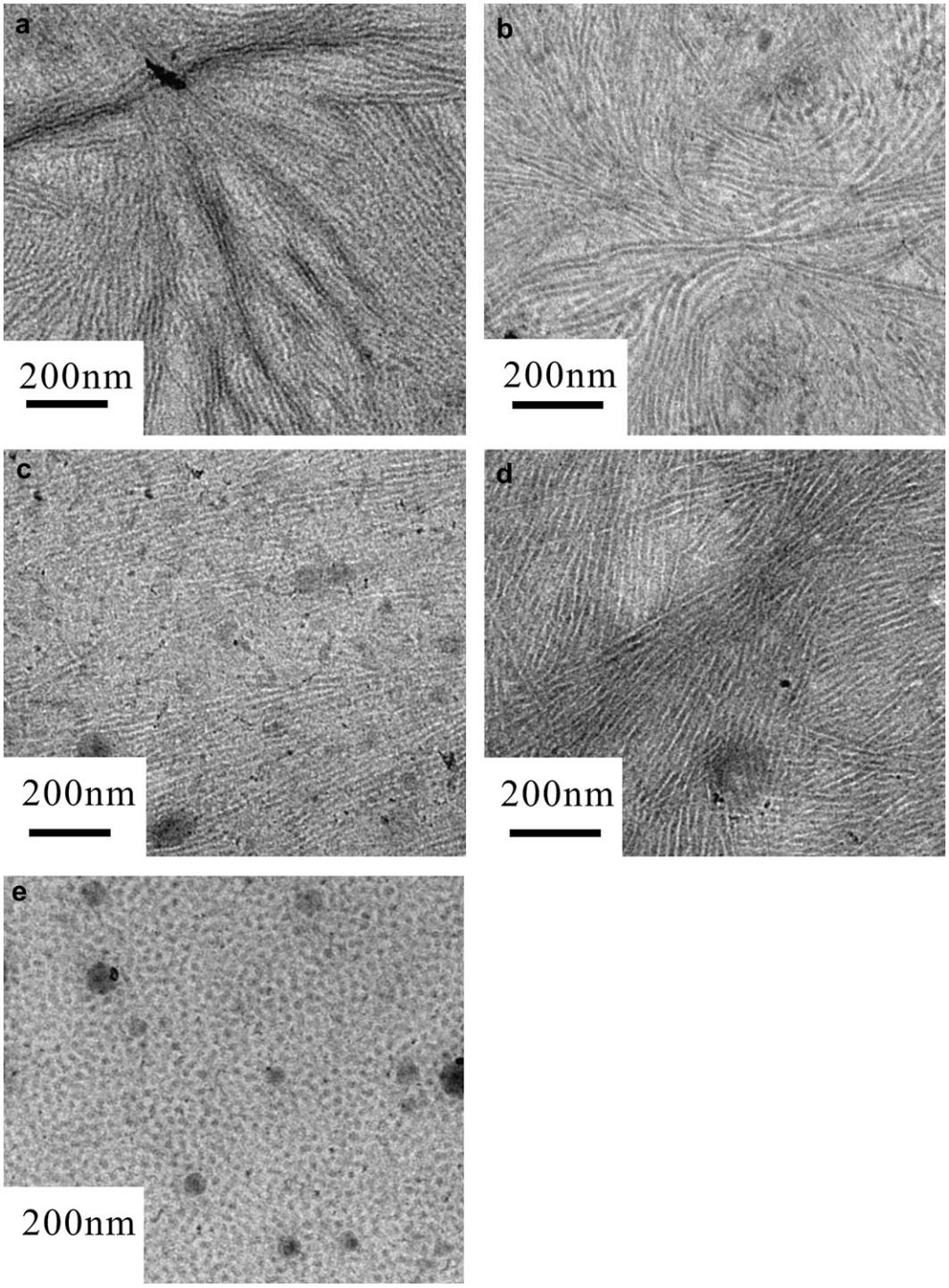

Fig. 5. TEM micrographs of triblock copolymers after melt crystallization treatment. (a) $La_{25}DM_{50}La_{25}$; (b) $La_{60}DM_{50}La_{60}$; (c) $La_{70}DM_{50}La_{70}$; (d) $La_{40}DM_{130}La_{40}$; (e) $La_{220}DM_{100}La_{220}$.

PDMS segments has a higher electron density than the oxygen atoms in PLLA and the high chain mobility of PDMS allows RuO_4 to diffuse into rubbery domains more readily than into the glass region of PLLA, the dark regions of the TEM micrograph in Fig. 1 represent the PDMS domains.

As can be seen in Fig. 1, the typical morphologies of these triblock copolymers, including lamellae, cylinders and spheres, were formed as determined by the M_w and PLLA/PDMS composition ratio of the triblock copolymers. Fig. 2(a) and Fig. 3(a) show the SAXS profiles of $La_{60}DM_{50}La_{60}$ and $La_{70}DM_{50}La_{70}$, obtained at room temperature, after they had been melted at by 10 °C above Tm and then quenched in the liquid nitrogen. The first- and higher-order diffraction peaks in the melting state show the position ratio of $1 : \sqrt{3} : \sqrt{7}$ for both specimens, suggesting that both triblock copolymers self-assembled into a cylindrical morphology, with the discrete cylindrical components of PDMS dispersed in the PLLA matrix. For the molten structure of $La_{220}DM_{100}La_{220}$, the SAXS curve in Fig. 4(a) reveals two shoulder diffraction peaks with the

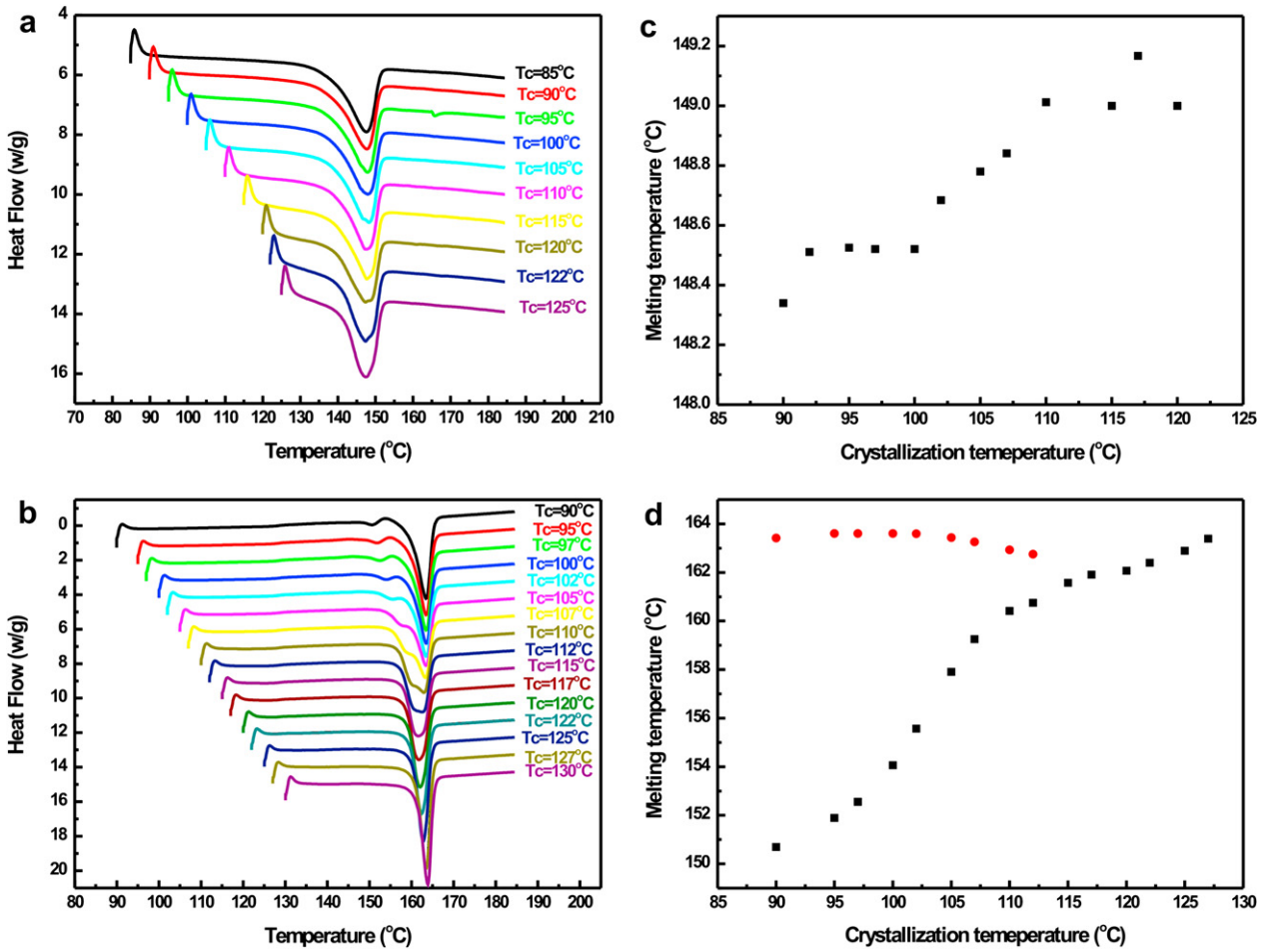

Fig. 6. Effect of crystallization temperature on the melting behavior of triblock copolymers (a) $La_{25}DM_{50}La_{25}$; (b) $La_{60}DM_{50}La_{60}$, and their corresponding relationship between T_c and T_m of triblock copolymers (c) $La_{25}DM_{50}La_{25}$; (d) $La_{60}DM_{50}La_{60}$.

position ratio of $1 : \sqrt{2} : \sqrt{3}$, indicating that a minor PDMS domain was present as a spherical structure within the matrix. These morphological patterns of the triblock copolymers were consistent with the phase diagram predicted by self-consistent field theory [32]. However, $La_{25}DM_{50}La_{25}$ exhibited a disordered structure rather than the predicted lamellar structure because the low degree of polymerization did not reach the weak segregation limit.

3.2. Effect of crystallization on morphology of triblock copolymers

Fig. 2(b) displays the SAXS profile of $La_{60}DM_{50}La_{60}$ that was crystallized at 120 °C for 30 min. It can be seen from Fig. 2 (b) that the periodic diffraction peaks that corresponded to the cylindrical structure were absent and the position ratio of the diffraction peaks was 1:2, indicating that the cylindrical morphology of $La_{60}DM_{50}La_{60}$ was disturbed and the crystallization induced the formation of lamellar structures, in a manner consistent with the TEM micrograph in Fig. 5(b), which displayed sheaf-like morphologies. Except disordered melt structure of $La_{25}DM_{50}La_{25}$, the cylinder domains comprised PLLA in $La_{40}DM_{130}La_{40}$ and PDMS in $La_{70}DM_{50}La_{70}$ rearranged through the break-out of the microphase-separated morphologies and the lamellar structures were formed, as shown in Fig. 5(a) for $La_{25}DM_{50}La_{25}$, Fig. 5(c) for $La_{70}DM_{50}La_{70}$ and Fig. 5 (d) for $La_{40}DM_{130}La_{40}$. For the case of $La_{220}DM_{100}La_{220}$, Fig. 4(b) presents the SAXS profile of $La_{220}DM_{100}La_{220}$ that was isothermally crystallized at 140 °C for 120 min; the fact that the scattering vector of crystallized $La_{220}DM_{100}La_{220}$ was the same as that of $La_{220}DM_{100}La_{220}$ in the melting state, demonstrating that the melting structure was retained upon crystallization, even though the higher-order diffraction peaks were absent [6,7,10,14,33]. This finding is consistent with the TEM micrograph.

The structure associated with the morphologies of the semi-crystalline block copolymers after crystallization was dominated by the competition between the crystallization procedure and the microphase separation. The Flory–Huggins interaction parameter χ of the block copolymers was estimated using the following equation [8]:

$$\chi = \frac{V_r(\delta_{PLLA} - \delta_{PDMS})^2}{RT}$$

where V_r is the molar segmental volume, and the solubility parameters of the PDMS (δ_{PDMS}) and PLLA (δ_{PLLA}) segments were approximately 15.6 $(J/cm^3)^{1/2}$ and 20.02 $(J/cm^3)^{1/2}$ [34,35], respectively. V_r was calculated as described in the previous literature [16]. The estimation of χN of the triblock copolymers in this article, except for $La_{220}DM_{100}La_{220}$, at by 10 °C above Tm ranged from 40.8 to 88.5, suggesting that these samples exhibited intermediate segregation strength ($10.5 < \chi N < 100$) according to the mean-field theory [36]. Consequently, the driving force of crystallization overwhelmed the intermediate segregation strength of these triblock copolymers, leading to the destruction of the molten morphologies of these triblock copolymers. Shiomi et al. found out

that the crystalline phase structures of poly(ethylene glycol)-poly(butadiene) diblock copolymers depended on the crystallization temperatures because the morphology changes on crystallization from microphase separation melts are governed by kinetics factor [14]. Comparing Fig. 1(f) with Fig. 5(e), the molten structure of $La_{220}DM_{100}La_{220}$ was preserved upon crystallization. The result could be attributed not only to its high segregation strength with χN of 239.5, but also to that the crystallization rate of PLLA might be higher than the diffusion rate of PLLA segment, leading to that the crystallization occurred preceding the structure rearrangement; hence PLLA segment crystallized in the origin microphase separation structure rather than in a rearranged one.

3.3. *Effect of isothermal crystallization on the melting behavior of PLLA–PDMS–PLLA*

The melting behavior of triblock copolymers was monitored using DSC after the specimens had been crystallized isothermally at distinct T_c. Fig. 6 shows the representative DSC thermodiagrams and melting temperatures of triblock copolymers $La_{25}DM_{50}La_{25}$ and $La_{60}DM_{50}La_{60}$ as a function of T_c over a wide range from 85 °C to 130 °C. As presented in Fig. 6 (b), $La_{60}DM_{50}La_{60}$ exhibited the double melting behaviors; Fig. 6(d) plots the dependence of the T_m on T_c for $La_{60}DM_{50}La_{60}$: the high T_m (T_{cH}) were almost unchanged with varying T_c as the T_c was below 105 °C, but the low Tm (Tm_L) increased continuously with T_c. Eventually, the unique Tm was observed when T_c was higher than 115 °C. Such double-melting behavior is commonly explained using the melting-recrystallization model [37–40]. The specimen $La_{60}DM_{50}La_{60}$ exhibited not only double melting behavior, but also a small exothermal signal, associated with the disorder-to-order transition (α' to α) of PLLA crystallite that was verified using FT-IR and WAXS [39–43].

Unlike $La_{60}DM_{50}La_{60}$ that exhibited complicated melting behavior, $La_{25}DM_{50}La_{25}$ yielded a single melting peak in the DSC traces, presented in Fig. 6(a), even though isothermal crystallization was conducted at low $T_c = 85$ °C. Fig. 7 (a) shows the WAXD patterns of $La_{25}DM_{50}La_{25}$ that was isothermal crystallized at various temperatures. The intense peaks that corresponding to (200/100) plane at $2\theta = 16.7°$ and (203) plane at 19.4° were present for all of the specimens, but the (015) reflection at 22.5° was observed only at high T_c. According to Zhang et al. [42], the packing of the side groups in the helical chains of the α'-form crystal is less ordered and looser than that of the α-form crystal, but both form have the same orthorhombic unit cell. Fig. 7(a) reveals that no obvious shift of the (200/100) and (203) diffraction peaks, indicating that the order of the chain packing was not influenced by the selected T_c. FT-IR spectra, which were highly-sensitive to the chain conformation and manner of packing of polymer chains, were also utilized to analyze the crystallite structure of $La_{25}DM_{50}La_{25}$. Fig. 7(b) shows the C=O stretching band of the PLLA segment for $La_{25}DM_{50}La_{25}$ crystallized at various T_c, and reveals that all of the specimens yield an absorption band at 1749 cm^{-1}, which was assigned to the α-form of PLLA crystallite [40–43]. Moreover, the characteristic diffraction peak near $2\theta = 24.5°$ from the PLLA α'-phase crystallite [40–43] was absent in Fig. 7(a) for all the specimens. These result demonstrated that the PLLA crystallite in $La_{25}DM_{50}La_{25}$ was present in the α form, as it was in $La_{40}DM_{130}La_{40}$. Fig. 8 presents the crystallite of PLLA homopolymer with M_w of 3000 (g/mol.) that was crystallized at distinct T_c. The strongest diffraction signal at $2\theta = 16.9°$ was the (200/100) plane. The shift of the diffraction of (203) from 19.1° to 19.4° with decreasing the selected T_c and the presence of the diffraction angle at 24.5° at

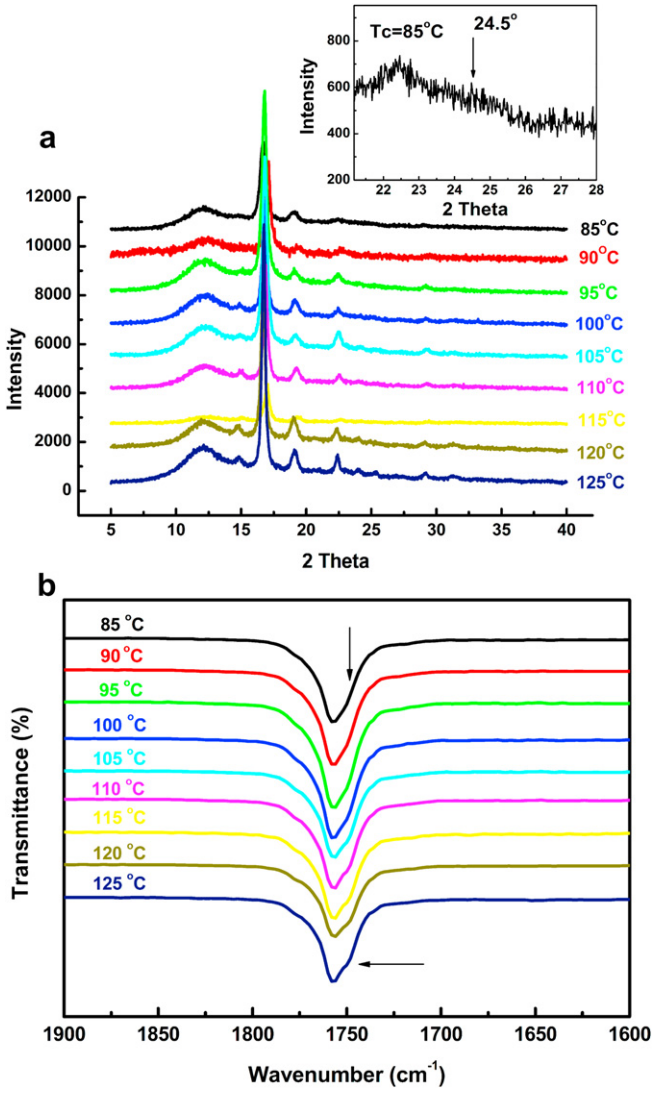

Fig. 7. (a) WAXD patterns and (b) FT-IR spectra of $La_{25}DM_{50}La_{25}$ crystallized at the selected temperature.

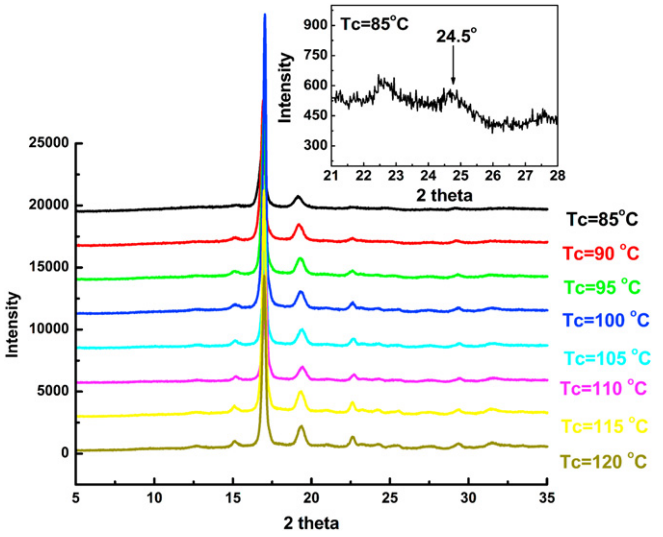

Fig. 8. WAXD patterns of PLLA with Mw of 3000 (g/mol.) that was crystallized at the selected temperature.

$T_c = 85$ °C indicates that the α′-phase crystallite was formed at low T_c. Therefore, it was inferred that the PDMS, as a major component in $La_{25}DM_{50}La_{25}$, partially dissolved in PLLA [31] and the mobility of PLLA was enhanced, facilitating the array of PLLA segments and formation of an ordered crystallite during the crystallization procedure (Fig. 8).

The equilibrium melting point (T_m^0) of the triblock copolymers was estimated by linear Hoffman–Weeks (HW) extrapolation of the curve of T_m versus T_c to the line $T_m = T_c$,

$$T_m = \frac{T_c}{\gamma} + T_m^0\left(1 - \frac{1}{\gamma}\right)$$

where γ is the thickening ratio [44]. Fig. 6(c) and (d) present the representative plot of T_m as a function of T_c for PLLA–PDMS–PLLA triblock copolymers. Since the complicated melting behavior of PLLA depends on T_c and the chemical composition, T_m^0 was estimated from value of T_{cL} that was obtained at $T_c > 110$ °C. Table 1 lists the equilibrium melting points of the triblock copolymers in this work, and shows that the T_m^0 increased with the chain length of the PLLA segments.

3.4. Dependence of crystallization rate on the chemical composition

Fig. 9(a) shows a representative plot of crystallization time versus relative crystallinity for PLLA homopolymer and PLLA–PDMS–PLLA triblock copolymers, from which the crystallization half-time ($t_{1/2}$), which corresponds to the time necessary for the specimens reach a relative crystallinity of 50%, can be taken as a characteristic parameter of the rate of crystallization. Fig. 9(b) plots the dependence of $t_{1/2}$ on the T_c for homopolymer and for the triblock copolymers that contain PLLA chain length of 5000 (g/mol.). As shown in Fig. 9(b), all $t_{1/2}$ values of the triblock copolymers in the range 95–125 °C exceeded that of the PLLA homopolymer, suggesting that introduction of soft PDMS segments reduced the crystallization rate. Besides the spatial discontinuity of crystalline domains resulting from the microphase separation, the rejection of the soft PDMS segments that were partially dissolved in the PLLA domains [31] from the crystallite growth front during the crystallization procedure further reduced the R_c of the triblock copolymers.

Fig. 10 plots the dependence of $t_{1/2}$ on the chemical composition of the triblock copolymers; the $t_{1/2}$ decreases as the chain length of PLLA segment in the triblock copolymers increases, suggesting that the M_w of PLLA in the trblock copolymers influenced the rate of crystallization. The Lauritzen and Hoffman theory provides the growth rate as follows [45,46]:

$$G \propto \exp\left(-\frac{Q_D}{k_B(T_C - T_D)}\right)\exp\left(-\frac{4b_0\sigma\sigma_e T_m^0}{k_B T_c \Delta h_f^0\left(T_m^0 - T_c\right)}\right)$$

where Q_D is the activation energy of the diffusion process in the crystallization; b_0 is the monomolecular thickness; σ and σ_e are the side and fold surface free energies, respectively; Δh_f^0 is the bulk enthalpy of melting per unit volume of crystal; T_m^0 is the equilibrium melting point, and T_0 is the temperature at which molecular diffusion is totally prohibited. The first and second terms of the above proportionality were associated with the chain mobility and the secondary nucleation, respectively, and the combined effect of these two factors determines the bell shape of the dependence of T_c on the growth rate. As described in Section 3.3, triblock copolymers that contained longer PLLA segments had higher T_m^0. Hence, for a given T_c, a triblock copolymer with higher PLLA Mw was crystallized at a higher degree of undercooling ($T_c - T_m^0$) and had a higher Rc. Furthermore, as described in the previous paragraph,

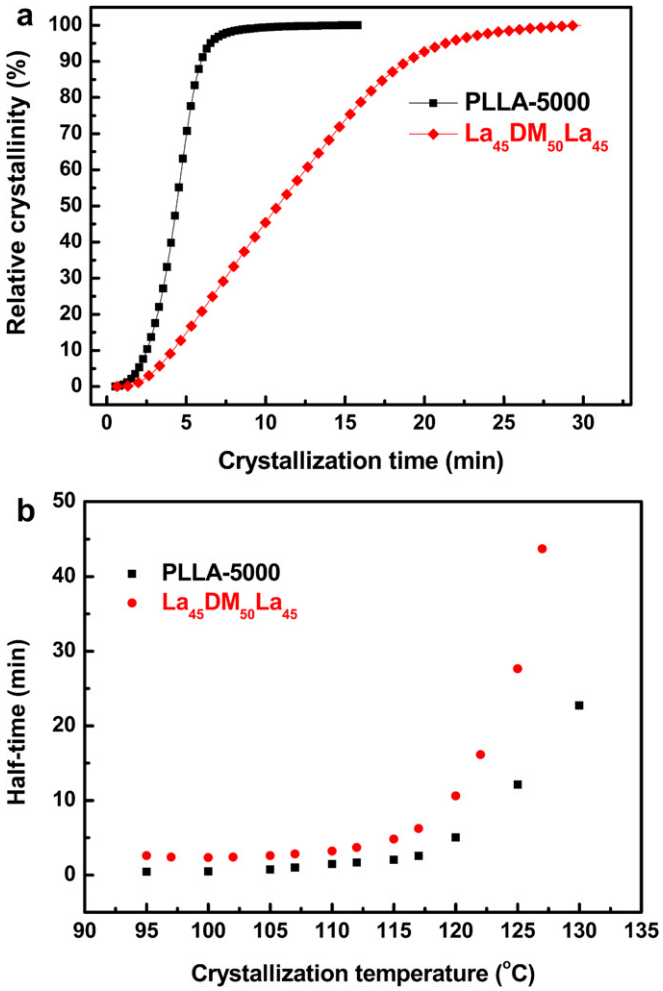

Fig. 9. (a) Plot of relative crystallinity as a function of crystallization time and (b) Plot of T_c versus $t_{1/2}$ for PLLA-5000 homopolymer and $La_{45}DM_{50}La_{45}$.

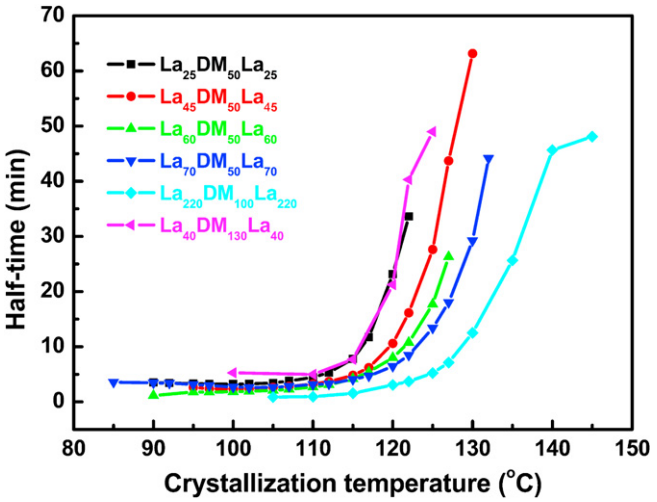

Fig. 10. Plot of T_c versus $t_{1/2}$ of triblock copolymers with various chemical compositions.

the introduction of PDMS segments inhibits the packing of PLLA segments and reduces the R_c of triblock copolymers. Hence, the increase in the weight fraction of PLLA in the triblock copolymers associated with the increase in the chain length of PLLA segments would decrease the effect of PDMS segments on the PLLA crystallization and further enhance the R_c of PLLA–PDMS–PLLA triblock copolymers. However, as in $La_{40}DM_{130}La_{40}$, the crystallizable blocks that were dispersed in the PDMS matrix suggested that the continuity of the crystalline region was disrupted by the amorphous regions, constraining the crystallization area and retarding the crystallization process.

4. Conclusion

In this work, the amorphous-semicrystalline triblock copolymers that comprised poly(L-lactide) and poly(dimethyl siloxane) were prepared, and their morphologies were characterized by SAXS and TEM. $La_{25}DM_{50}La_{25}$ showed disordered melts due to their low segregation strength. The melting morphologies changed from lamellar to spherical structures as the molecular weight of the triblock copolymers increased, in a manner depended on the volume fraction of PLLA in the triblock copolymers. The SAXS profiles and TEM micrographs of the triblock copolymers in the solid state revealed the break-out of the molten structures. However, the molten morphology of $La_{220}DM_{100}La_{220}$ was preserved because it possessed strong segregation strength.

The effect of isothermal crystallization on the melting behaviors was investigated using DSC, WAXS and FT-IR. Except for $La_{25}DM_{50}La_{25}$ which had a unique melting point, all of the specimens exhibited the double-melting behaviors that were associated with the recrystallization-melting mechanism. The crystallite of $La_{25}DM_{50}La_{25}$ formed at various T_c was identified using WAXS and FT-IR. The presence of the IR absorption at 1749 cm^{-1} associated with the α phase of PLLA crystallite and the absence of diffraction angle at $2\theta = 24.5^\circ$ attributed to the PLLA α'-phase crystallite suggest that the unique α phase of PLLA crystallite formed even though the T_c was below 90 °C. The enhancement of the chain mobility may have promoted the package of the PLLA chains and the formation of the ordered PLLA α-phase crystallite.

The isothermal crystallization kinetics, investigated by DSC, showed that the crystallization rate (R_c) of triblock copolymers was less than that of PLLA homopolymers. With respect to the effect of the chemical composition of the triblock copolymers on their R_c, a higher chain length of PLLA in the block copolymer exhibited a higher R_c because of the larger degree of undercooling ($T_c - T_m^0$). However, $La_{40}DM_{130}La_{40}$ with PLLA as minor component had a significantly lower R_c than that contained PLLA as the major phase because the PDMS matrix disrupted the continuity of the crystallizable domains, increasing the difficulty of the crystallite growth and reducing probability of the crystallization of its neighboring domains.

Acknowledgements

The authors would like to thank the Industrial Technology Research Institute of Taiwan, for financially supporting this research. Dr. Ren-Jye Wu of the Industrial Technology Research Institute of Taiwan, and Prof. Yan-Jyi Huang of National Taiwan University of Science and Technology are appreciated for the help of the SAXS experiment.

References

[1] Loo YL, Register RA, Ryan AJ, Dee GT. Macromolecules 2001;34(26):8968–77.
[2] Xu JT, Yuan JJ, Cheng SY. European Polymer Journal 2003;39(11):2091–8.
[3] Lorenzo AT, Arnal ML, Muller AJ, Boschetti-de-Fierro A, Abetz V. Macromolecules 2007;40(14):5023–37.
[4] Schmalz H, Knoll A, Muller AJ, Abetz V. Macromolecules 2002;35(27):10004–13.
[5] Rangarajan P, Register RA, Fetters LJ. Macromolecules 1993;26(17):4640–5.
[6] Ho RM, Chung TM, Tsai JC, Kuo JC, Hsiao BS, Sics I. Macromolecular Rapid Communications 2005;26(2):107–11.
[7] Castillo RV, Muller AJ, Lin MC, Chen HL, Jeng US, Hillmyer MA. Macromolecules 2008;41(16):6154–64.
[8] Tzeng FY, Lin MC, Wu JY, Kuo JC, Tsai JC, Hsiao MS, et al. Macromolecules 2009;42(8):3073–85.
[9] Ho RM, Lin FH, Tsai CC, Lin CC, Ko BT, Hsiao BS, et al. Macromolecules 2004;37(16):5985–94.
[10] Loo YL, Register RA, Ryan AJ. Macromolecules 2002;35(6):2365–74.
[11] Rangarajan P, Register RA, Adamson DH, Fetters LJ, Bras W, Naylor S, et al. Macromolecules 1995;28(5):1422–8.
[12] Ryan AJ, Hamley IW, Bras W, Bates FS. Macromolecules 1995;28(11):3860–8.
[13] Cohen RE, Cheng PL, Douzinas K, Kofinas P, Berney CV. Macromolecules 1990;23(1):324–7.
[14] Shiomi T, Takeshita H, Kawaguchi H, Nagai M, Takenaka K, Miya M. Macromolecules 2002;35(21):8056–65.
[15] Shiomi T, Tsukada H, Takeshita H, Takenaka K, Tezuka Y. Polymer 2001;42(11):4997–5004.
[16] Zhu L, Cheng SZD, Calhoun BH, Ge Q, Quirk RP, Thomas EL, et al. Polymer 2001;42(13):5829–39.
[17] Hamley IW, Fairclough JPA, Terrill NJ, Ryan AJ, Lipic PM, Bates FS, et al. Macromolecules 1996;29(27):8835–43.
[18] Quiram DJ, Register RA, Marchand GR. Macromolecules 1997;30(16):4551–8.
[19] Hamley IW, Parras P, Castelletto V, Castillo RV, Muller AJ, Pollet E, et al. Macromolecular Chemistry and Physics 2006;207(11):941–53.
[20] Ryan AJ, Fairclough JPA, Hamley IW, Mai SM, Booth C. Macromolecules 1997;30(6):1723–7.
[21] Loo YL, Register RA, Adamson DH. Macromolecules 2000;33(22):8361–6.
[22] Drumright RE, Gruber PR, Henton DE. Advanced Materials 2000;12(23):1841–6.
[23] Auras R, Harte B, Selke S. Macromolecular Bioscience 2004;4(9):835–64.
[24] Ho CH, Wang CH, Lin CI, Lee YD. Polymer 2008;49(18):3902–10.
[25] Yan SF, Yin JB, Yang Y, Dai ZZ, Ma J, Chen XS. Polymer 2007;48(6):1688–94.
[26] Oyama HI. Polymer 2009;50(3):747–51.
[27] Jiang L, Wolcott MP, Zhang JW. Biomacromolecules 2006;7(1):199–207.
[28] Lee JK, Kim MR, Lee HJ, Chung I, Lim KT, Jeon S, et al. Wiley-V C H Verlag Gmbh. p. 91–6.
[29] Ragheb RT, Riffle JS. Polymer 2008;49(25):5397–404.
[30] Kricheldorf HR, Rost S, Wutz C, Domb A. Macromolecules 2005;38(16):7018–25.
[31] Ho CH, Wang CH, Lin CI, Lee YD. European Polymer Journal 2009;45(8):2455–66.
[32] Matsen MW, Thompson RB. Journal of Chemical Physics 1999;111(15):7139–46.
[33] Zhu L, Mimnaugh BR, Ge Q, Quirk RP, Cheng SZD, Thomas EL, et al. Polymer 2001;42(21):9121–31.
[34] Yilgor E, Yilgor I. Polymer 2001;42(19):7953–9.
[35] Garlotta D. Journal of Polymers and the Environment 2001;9(2):63–84.
[36] Matsen MW, Bates FS. Macromolecules 1996;29(4):1091–8.
[37] He Y, Fan ZY, Hu YF, Wu T, Wei J, Li SM. European Polymer Journal 2007;43(10):4431–9.
[38] Yasuniwa M, Tsubakihara S, Sugimoto Y, Nakafuku C. Journal of Polymer Science, Part B: Polymer Physics 2004;42(1):25–32.
[39] Yasuniwa M, Lura K, Dan Y. Polymer 2007;48(18):5398–407.
[40] Pan PJ, Zhu B, Kai WH, Dong T, Inoue Y. Macromolecules 2008;41(12):4296–304.
[41] Zhang J, Tashiro K, Tsuji H, Domb AJ. Macromolecules 2008;41(4):1352–7.
[42] Zhang JM, Duan YX, Sato H, Tsuji H, Noda I, Yan S, et al. Macromolecules 2005;38(19):8012–21.
[43] Pan P, Kai W, Zhu B, Dong T, Inoue Y. Macromolecules 2007;40(19):6898–905.
[44] Hoffman JD, Weeks JJ. Journal of Research of the National Bureau of Standards Section A-Physics and Chemistry 1962;66(JAN-F):13.
[45] Hoffman JD. Polymer 1982;23(5):656–70.
[46] Hoffman JD. Polymer 1983;24(1):3–26.